ELSEVIER

Space and time-resolved gene expression experiments on cultured mammalian cells by a single-cell electroporation microarray

Research Paper

S. Vassanelli[1], L. Bandiera[2], M. Borgo[2], G. Cellere[3], L. Santoni[2], C. Bersani[2], M. Salamon[4], M. Zaccolo[5], L. Lorenzelli[6], S. Girardi[1], M. Maschietto[1], M. Dal Maschio[1,7] and A. Paccagnella[3]

[1] University of Padova, Department of Human Anatomy and Physiology, Section of Physiology, via Marzolo 3 – 35131, Padova, Italy
[2] Narvalus s.r.l., Bioindustry Park Canavese, via Ribes 5 – 10010, Colleretto Giacosa, Torino, Italy
[3] University of Padova, Department of Electronic Engineering, via Gradenigo 6/B – 35131, Padova, Italy
[4] University of Padova, CRIBI Biotechnology Centre, viale G. Colombo 3 – 35121, Padova, Italy
[5] Venetian Institute for Molecular Medicine (VIMM), via Orus 2 – 35129, Padova, Italy
[6] Fondazione B. Kessler, via Sommarive 18 – 38050, Povo, Trento, Italy
[7] IIT, Italian Institute of Technology, via Morego 30 – 16163, Genova, Italy

Single-cell experiments represent the next frontier for biochemical and gene expression research. Although bulk-scale methods averaging populations of cells have been traditionally used to investigate cellular behavior, they mask individual cell features and can lead to misleading or insufficient biological results. We report on a single-cell electroporation microarray enabling the transfection of pre-selected individual cells at different sites within the same culture (space-resolved), at arbitrarily chosen time points and even sequentially to the same cells (time-resolved). Delivery of impermeant molecules by single-cell electroporation was first proven to be finely tunable by acting on the electroporation protocol and then optimized for transfection of nucleic acids into Chinese Hamster Ovary (CHO-K1) cells. We focused on DNA oligonucleotides (ODNs), short interfering RNAs (siRNAs), and DNA plasmid vectors, thus providing a versatile and easy-to-use platform for time-resolved gene expression experiments in single mammalian cells.

Introduction

A major challenge of modern genetic research is to decipher how genes and their control elements within the mammalian genome operate together to perform physiological, developmental, and pathological responses in the living cell. Single-cell experiments represent a valuable work-bench to address the issue. Although many advances have been achieved in the past decades investigating cell populations as a whole by molecular biology techniques, one major new paradigm in gene expression is that it varies stochastically among different individual cells, thus implying that population analysis may be misleading [1–3]. In fact, DNA, many mRNA molecules and some enzymes exist in low copy numbers and participate in stochastic reaction events that are often at non-equilibrium steady state, thus causing gene expression to vary from cell to cell even within very homogenous populations [4–6]. Furthermore, when dealing with intact tissues or primary cultures from animals, cells of different type or differentiation stage coexist and interact within the same experimental sample. A textbook example is represented by neurons where gene expression events are related to the individual cell type and depend on complex signaling within neuronal networks [7]. On this basis, it is clear that a thorough understanding of gene expression mechanisms and cell behavior requires efficient methods for the investigation of molecular processes in single cells rather than in a population where averaging hides stochasticity and individual cell properties.

A comprehensive single-cell experimental approach should combine the possibility to both detect and manipulate genetic

Corresponding author: Vassanelli, S. (stefano.vassanelli@unipd.it)

1871-6784/$ - see front matter doi:10.1016/j.nbt.2008.03.002

events in the target cell. Many recent studies have been focused on the development of new techniques for monitoring gene expression. Part of them draw upon the unique capabilities of molecular probes to track the fate of mRNAs and proteins in time-lapse fluorescence microscopy experiments [8–12], thus offering the possibility to investigate the dynamics of gene expression down to a single molecule resolution. Other approaches rely, instead, on the application to single cells of molecular biology and biochemical techniques such as the reverse transcription-polymerase chain reaction (RT-PCR) [6,13], DNA-microarray analysis [14], and electrophoresis-based molecules separation [15]. On the contrary, the molecular tools to manipulate gene expression in living cells are in continuous development: DNA plasmid vectors to express exogenous genes; antisense molecules, such as oligodeoxyribonucleotides (ODNs), ribozymes, DNAzymes, and, most recently, interfering RNAs and peptide nucleic acids (PNAs), to knockdown gene expression [33]; decoy ODNs, to control nuclear transcription factors [16]; zinc finger nucleases (ZFNs) [17,18,19] or specifically engineered ODNs with locked nucleic acids [48], for site directed mutagenesis, and gene editing. Despite the availability of this rich molecular toolbox to monitor and manipulate gene expression in the living cell, single-cell delivery remains a major problem to tackle. Traditional delivery techniques, such as chemical or viral transfection, suffer, in this respect, major constraints: (i) they act on entire cell populations and not on individual cells; (ii) they work only with certain cell types and molecules. An alternative is represented by electroporation: the application of large voltages to the cells generates transient pores in the plasma membrane, thereby allowing the permeation of a large variety of molecules, from small ions to genetic constructs and proteins, to a broad range of cells, from cell lines to primary cells [20]. Although the method has the advantage to operate with different molecules and cell types, it is traditionally applied only to populations of cells. In fact, electroporation is usually carried out in cuvettes, thus sharing with other bulk-scale methods the averaging limitation and requiring cell harvesting and re-suspension for cells that are growing in adhesion, which destroys original cell–cell connections. Even in the case of '*in situ*' electroporation, an advanced implementation where adherent cells are electroporated on millimeter-scale indium-tin-oxide (ITO)-coated glass slides [21], only large cell populations can be addressed. The development of new versatile single-cell molecular delivery approaches represents, therefore, a very useful and fundamental challenge.

Efficient single-cell delivery was achieved by using carbon fiber microelectrodes or glass micropipettes capable to produce membrane electroporation [22]. Such devices, however, are difficult to handle and can be hardly implemented into large-scale systems. To overcome these limitations, silicon microchips for single-cell electroporation have been recently developed, for example using a sort of miniaturized electroporation chamber or a microfluidic channel [22], thus paving the way to large-scale integration. In turn, these systems rely on a rather complex fabrication process and are working only on cells in suspension, which is a serious drawback for the treatment of most mammalian cells in culture that are typically growing in adhesion on a solid substrate.

In this work, we report on a new single-cell delivery technology based on a silicon chip featuring an array of cell-sized planar microelectrodes. The cells, growing in adhesion on the chip surface as on a conventional glass coverslip, were individually electroporated by imposing on the single microelectrodes appropriate voltage transients. In this way, impermeant molecules present in the extracellular medium were delivered to pre-selected target cells. Coupled to a PC driven control system capable to arbitrarily design the voltage protocols and to address independently the single electrodes, the chip was allowing a tunable delivery of molecules to individual cells with a fine control over the cell membrane permeability to the different compounds. Moreover, molecules could be delivered to cells located at different sites within the same culture (space-resolved), at arbitrarily chosen time points (time-resolved), and even sequentially to the same cell (serial delivery). The technique was successfully tested for delivery to CHO-K1 cells of several nucleic acids, ranging from ODNs to siRNAs and DNA plasmid vectors, thereby achieving the single-cell expression and silencing of fluorescent reporters. Thus, the approach is proposed as a new easy-to-use platform to perform space and time-resolved gene expression experiments in single cultured mammalian cells.

Materials and methods

Single-cell electroporation array and control system

Figure 1a shows schematically the building blocks of the experimental setup. The key element of the system was a chip featuring an array of 60 cell-sized microelectrodes enabling single-cell electroporation. This silicon microchip was fabricated following a custom design and using the adaptation of the backend of a CMOS (complementary metal–oxide–semiconductor) process by ITC-irst, Povo-Trento, Italy. The array of 60 circular microelectrodes was integrated on the die. The metal lines connecting the electrodes to the external circuitry and the free silicon surface were insulated from the extracellular electrolyte by deposition of a layer (200 nm) of amorphous silicon nitride (Si_3N_4). The active area of the electrodes was realized with a gold layer and its diameter, which was identical among electrodes of the same chip, ranged between 15 and 50 μm to match different sizes of different cell types. The distance between the electrodes was either 150 or 300 μm depending on chip design. To build a complete BioChip, one silicon chip was encased in a custom package for connection to the control system (see below), and included a plastic culture chamber (4 mm inner diameter) attached to the chip surface in order to contain the medium for cell culture and the electroporation buffer (minimum volume 50 μl, maximum volume 1 ml).

The microelectrodes array was addressed by using a custom-made switching system, and voltages were applied by a commercial function generator (Agilent 33220A, Agilent Technologies Inc., Palo Alto, CA, U.S.A.). The whole system was controlled by a personal computer running a LabVIEW-based software (National Instruments Corporation, Austin, TX, U.S.A.). In this way, each single microelectrode was independently addressed, thus allowing for the arbitrary choice of different combinations of electrodes and, for each electrode, the timing of electroporation.

Figure 1b represents the schematic of the equivalent electric circuit of a single cell on a microelectrode [23]. Here, only passive components of the cell membrane were considered and voltage-dependent channels were omitted since their contribution to the current flow through the membrane when compared to capacitive currents was negligible in our experimental conditions.

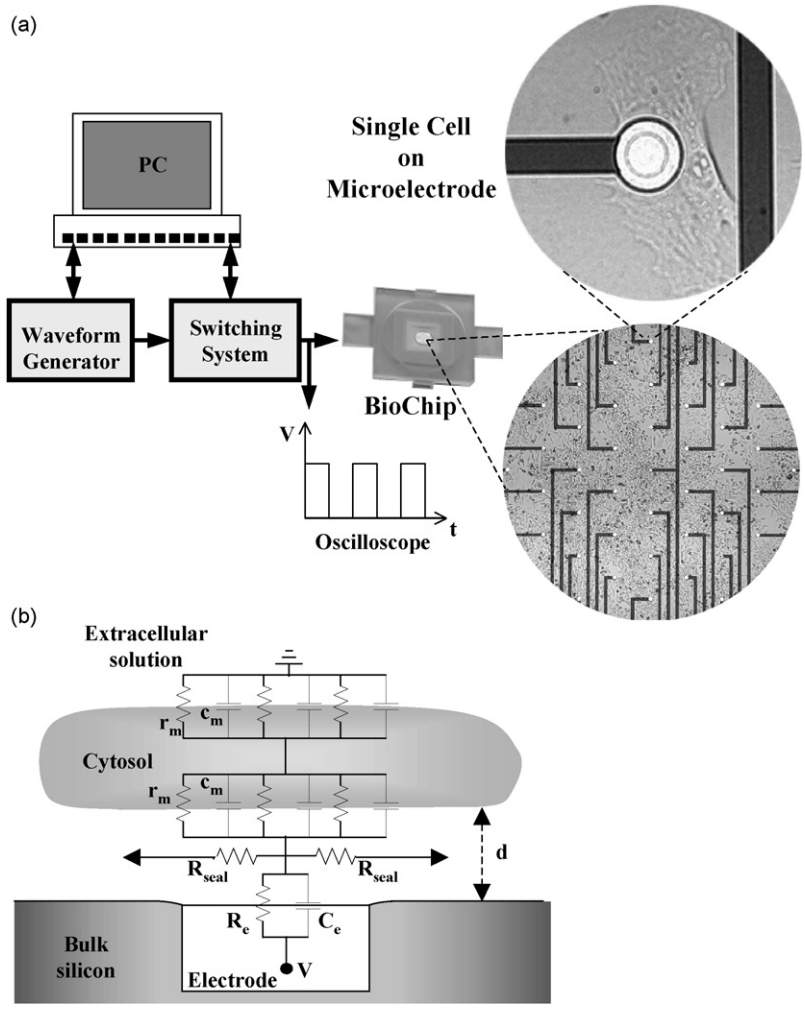

FIGURE 1

Chip and control system. (a) Schematics of a BioChip featuring the single-cell electroporation microarray and its control system driven by a personal computer. The control system allows, through a waveform generator and a switching system, to arbitrarily design voltage transients and to address independently each of the 60 microelectrodes of the array for single-cell electroporation. On the right side: micrograph of a culture of CHO-K1 cells on chip (right bottom). *Right-top*: magnification of a single cell growing in adhesion on one of the cell-sized electrodes (electrode diameter 15 μm. (b) Cross section of a cell growing in adhesion on a microelectrode and equivalent electrical model describing the coupling between cell and chip (not to scale). The circuit impedance depends on the electrode impedance (i.e. R_e, C_e), the resistance between the electrode and the bulk extracellular solution due to the thin layer of electrolyte (layer thickness *d*) separating the cell and the solid substrate (R_{seal}), the membrane capacitance (c_m) and the membrane resistance (r_m). Note that r_m is only a "passive" resistance considering that ion channels in CHO-K1 cells are nearly absent. The circuit accounts for the large capacitive current flowing through the cell membrane when fast voltage transients (*V*) are applied to the microelectrode, thus resulting in large voltage transients across the cell membrane and electroporation. The opening of pores temporarily shunts the cell interior to the zero potential of the grounded electrolyte.

Cell culture on chip

Chips were wiped carefully and rinsed with deionized water and sterilized with U.V. light or ethanol at 70 °C before each cell culture. Chinese hamster ovary cells K1 subclone (CHO-K1), wild-type or stably transfected with the ECFP reporter gene, were routinely maintained in Nutrient Mixture F-12 HAM (Sigma–Aldrich, St. Louis, MO, U.S.A.) supplemented with 10% heat-inactivated fetal bovine serum (FBS) (Sigma–Aldrich), 100 U/ml penicillin and 100 μg/ml streptomycin (Sigma–Aldrich) at 37 °C in a humidified atmosphere with 5% CO_2. Cells were trypsinized and replated on non-coated chips at a density of 80×10^3 cells/cm^2.

Nucleic acids

Fluorescent single-stranded ODNs (24 nt) were purchased from Sigma–Aldrich (Sigma-Genosys) (F indicates a 5′ end-conjugated Fluorescein: 5′-FCGCCGCGCGAATTCTGTCGGGGCG-3′, 5′-CGCCCCGACAGAATTCGCGCGGCG-3′). A double-stranded fluorescein labeled oligonucleotide (24 bp) was prepared by annealing the two complementary sequences and the formation of the double stranded ODN was checked by subsequent gel electrophoresis. The 24 bp double-stranded siRNA for ECFP silencing was purchased by Ambion, Austin, TX, U.S.A. (sense: 5′-GCAAGCUGACCCUGAAGUUCAUU-3′ antisense: 5′-GAACUUCAGGGUCAGCUUGCCGUU-3′). Its silencing effect on the EGFP gene in mammalian cell lines was previously reported [24]; in control experiments, we checked for ECFP silencing in populations of stably transfected CHO-K1 cells by using the Metafectene transfection reagent (Biontex Laboratories GmbH, Muenchen, Germany) for siRNA delivery according to manufacturer's instructions.

The EGFP, EYFP and ECFP cDNAs were independently cloned into the pcDNA3.1(-) vector (Invitrogen, Carlsbad, CA, U.S.A.) downstream to the CMV promoter for experiments of transient

transfection of cells. The concentration of the different nucleic acids was determined by ultraviolet (UV) absorption spectroscopy using a DU Series 500 spectrophotometer (Beckman Coulter Inc., Fullerton, CA, U.S.A.). Control experiments of transfection of cell populations with EGFP were performed using the Metafectene transfection reagent (Biontex Laboratories GmbH) according to the manufacturer's instructions.

Electrophysiology

Patch clamp pipettes were pulled from borosilicate glass capillaries (GB150T-10, Science Products GMBH, Hofheim, Germany) using a three stages puller (P-97, Sutter Instrument Co., Novato, CA, U.S.A.), fire-polished and coated with Sylgard (Sylgard, Dow Corning Co., Midland, MI, U.S.A.). Pipettes resistances in the recording solution were 1–3 MΩ and, after entering whole-cell configuration, only experiments with access resistance below 20 MΩ were considered. The pipette filling solution was in mM: 140 KCl, 1 $CaCl_2$, 2 $MgCl_2$, 10 EGTA, 5 HEPES, adjusted to pH 7.3 with KOH 1N. The extracellular recording solution was: 135 NaCl, 5.4 KCl, 1.8 $CaCl_2$, 1 $MgCl_2$, 10 D-glucose, 5 mM HEPES, adjusted to pH 7.4 with NaOH 1N. A Ag/AgCl reference electrode was used. Recordings of intracellular voltages were performed in whole-cell configuration and current-clamp mode using a single-electrode amplifier (SEC-10L, npi electronic GMBH, Tamm, Germany) controlled by a computer running a homemade data acquisition program based on a LabVIEW software (National Instruments Corporation).

Single-cell electroporation and delivery of molecules

Before electroporation, cells on the biochip were rinsed with PBS (in mM: 137 NaCl, 2.7 KCl, 10 Na_2HPO_4, 2 KH_2PO_4; pH 7.4) or with a high ionic strength buffer (buffer 1); then, the inner part of the culture chamber was filled with 25–50 μl of the electroporation solution that was kept to ground potential by reference electrodes integrated in the chip. For molecular delivery experiments, the electroporation solution was obtained by solubilization of the molecules to be delivered in PBS or buffer 1 at the following concentrations: Lucifer Yellow (LY) (Sigma–Aldrich), 1 mM; Trypan Blue (TB) (Sigma–Aldrich), 1 mM; Fluorescein labeled ODNs (Sigma–Aldrich), 100 nM-5 μm; control fluorescent siRNA (Ambion), 100 nM; ECFP-siRNA (Ambion), 50 nM; pcDNA3.1-EGFP (-EYFP, -ECFP), 1 μg in 25 μl of PBS or electroporation buffer 1. After electroporation and incubation for 1–10 min at room temperature, cells were washed with PBS prior observation. In the case of viability, gene expression, silencing and serial transfection experiments, 800 μl of culture medium pre-warmed to 37 °C were added to the culture chamber, the biochip placed into a petri dish and then kept at 37 °C in a humidified atmosphere with 5% CO_2. Before microscopy, the cells were rinsed twice with PBS.

Efficiency of delivery (E) was computed according to the following equation: $E = N^+/(N^- + N^+) \times 100$ where N^+ was the number of cell–microelectrode sites positive for molecular uptake while N^- was the number of negative sites. Accordingly, $N = N^+ + N^-$ was the total number of individual microelectrodes addressed on the single-cell electroporation array. Cell viability for a given voltage protocol was tested at 12–24 h by incubation for 1 min with a 1 mg/ml Trypan Blue solution in PBS in order to check for membrane integrity. Following the nomenclature used for the efficiency estimate the percentage of cell viability (V) was computed as following: $V = N^-/(N^- + N^+) \times 100$ (where N^- and N^+ indicate the number of sites negative and positive for TB uptake, respectively).

The non-specific uptake index (NS) was obtained from the ratio of positive cells located off-site and the positive cell–microelectrodes sites: $NS = (N^O/N^+) \times 100$, where N^O indicates the number of positive non-specific cells. For the determination of N^O, cells were counted around each stimulated electrode within one inter-electrodes distance (i.e. 150 or 300 μm).

For statistical evaluation on molecular delivery (see Results, Figure 4 and Table 1), several experimental trials (n) of $N = 100$ cell–microelectrode sites each were performed. To obtain a total number of 100 sites per trial, 5–8 chips were used in sequence for single-cell electroporation and delivery as described above. Complete trials were lasting 1–2 h, including microscopy and image capturing.

Microscopy

Cell uptake of dyes, fluorescent labeled nucleic acids, EGFP, EYFP, ECFP expression and ECFP silencing were observed using a microscope with epi-illumination for Brightfield and epi-fluorescence microscopy DM LB2, Leica Microsystems, Wetzlar, Germany (objectives: N PLAN 5X/0.12 and HCX PL APO L 20X/0.50 W U-V-I D3.5; filters sets: GFP and H3) or an Axioskope 40, Carl Zeiss AG, Germany (objectives: A-plan 5×/0.12 and Achroplan 20×/0.45 Ph2; filters

TABLE 1

Evaluation of non-specific uptake

	LY					TB					ODN				
	N^+	N^-	N^O	E	NS	N^+	N^-	N^O	E	NS	N^+	N^-	N^O	E	NS
Experiment 1	100	0	25	100	25.0	94	6	6	94	6.4	80	20	16	80	20.0
Experiment 2	93	7	14	93	15.1	100	0	8	100	8.0	81	19	15	81	18.5
Experiment 3	100	0	13	100	13.0	88	12	12	88	13.6	85	15	15	85	17.6
Experiment 4	82	18	6	82	7.3	77	23	12	77	15.6	72	28	10	72	13.9
Mean	93.8	6.3	14.5	93.8	15.1	89.8	10.3	9.5	89.8	10.9	79.5	20.5	14.0	79.5	17.5
S.D.	8.5	8.5	7.9	8.5	7.4	9.8	9.8	3.0	9.8	4.4	5.4	5.4	2.7	5.4	2.6

The table reports the values of positive cell–microelectrode sites, N^+, negative cell–microelectrode sites, N^-, positive off-site cells, N^O, efficiency, E, and non-specific uptake index, NS (see Material and Methods for exact definition and calculation), obtained with the three probe compounds LY, TB and ODN. Different rows report the results of four experimental trials (Experiments 1–4), each with 100 cell–microelectrode sites ($N = 100$). Arithmetical mean ($n = 4$) and standard deviation are reported for each parameter in the last two rows. Electroporation voltage protocol: 3 trains of 5, 10 ms wide, voltage pulses spaced by 100 ms (1.68 V amplitude).

sets: 06 and 34) or a BX51WI microscope, Olympus, Japan, (objectives: LumPlanFl water immersion 40× NA = 0.8 and LumPlanFl water immersion 10× NA = 0.3; filter sets for ECFP, EYFP and TRITC) while images were acquired by a DS-5MC (Nikon, Tokyo, Japan) or a DFC350FX (Leica Microsystems, Wetzlar, Germany) digital camera and stored on a PC.

Results

Single-cell electroporation on cell-sized microelectrode

A single-cell growing in adhesion on a cell-sized microelectrode represents a well-defined system where voltages applied to the microelectrode and their transfer to the cell membrane can be precisely controlled. The tight adhesion contact between a cell and a solid semiconductor substrate, with a distance that is typically in the order of a few tens of nanometers, ensures a strong electrical coupling between the single cell and the microelectrode [25]. As 'proof of principle', we investigated whether a single CHO-K1 cell growing in adhesion on a cell-sized planar microelectrode could be individually electroporated. In order to carefully analyse the membrane permeabilization process, the issue was first addressed by electrophysiological means with the cell that was contacted by a patch-clamp pipette in whole-cell configuration for intracellular potential recording. Upon application of a train of 10 ms wide voltage pulses to the microelectrode, the intracellular potential recorded by the patch-clamp pipette was undergoing a sudden transition, from a resting value of about −70 mV to 0 (Figure 2a). These changes of intracellular potential can be explained on the basis of a simple equivalent electrical model describing the coupling of the cell to the electrode and to the extracellular solution (Figure 1b). The thin layer of electrolyte separating the cell and the adhesion substrate represents an electrical resistance (several MΩ) that 'seals' the cleft from the grounded electrolyte [25]. Owing to the seal resistance, the application of fast voltage transients to the microelectrode caused the development of fast and large voltage transients in the cell membrane and the consequent opening of pores by an electroporation process. Pores opening temporarily shunted the intracellular potential to the grounded potential of the extracellular solution, thus causing the transition from −70 mV to 0. Shortly after (about 1.5 min), pores resealing allowed the smooth recovery of the cell to its resting potential (Figure 2b). Notably, the amplitude of the voltage applied to the microelectrode (1.3 V) was rather small when compared with traditional electroporation protocols for a population of cells in a cuvette, where hundreds or even thousands of volts are customarily used [20]. This was in agreement with the tight electrical coupling existing between the single cell and the microelectrode and in line both with previous impedance measurements [26] and with electroporation experiments performed on populations of cells adhering to large electrodes [27]. We verified the formation of membrane pores by observing the cell uptake of Lucifer Yellow, a low molecular weight (457 Da) fluorescent probe impermeable to the plasma membrane. Figure 3 shows a culture of CHO-K1 cells on a chip where a single cell in contact with a microelectrode was stimulated in the presence of LY in the extracellular solution. After washing, only the target cell was stained, thus demonstrating the opening of membrane pores and the possibility to deliver a compound into a pre-selected single-cell within a population.

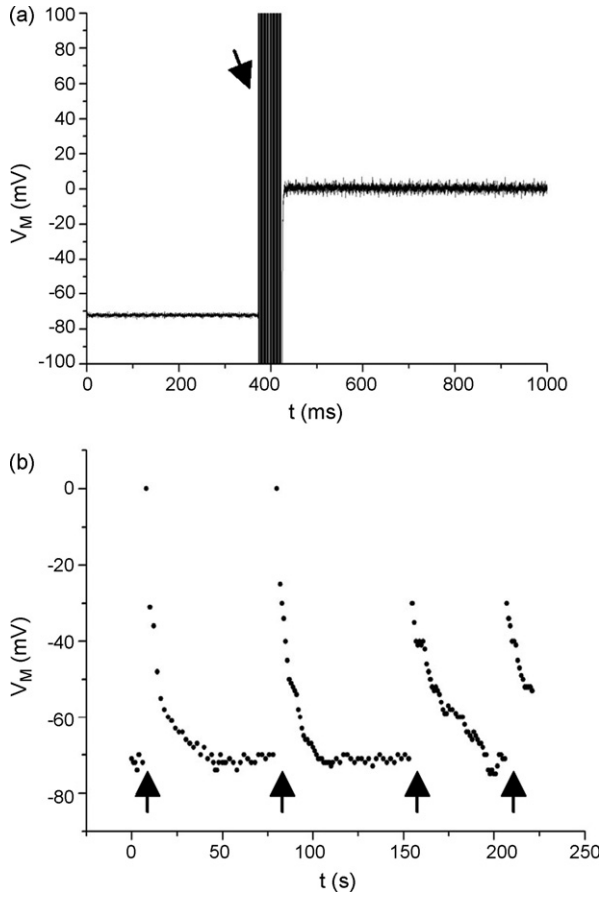

FIGURE 2

Intracellular potential of a CHO-K1 cell during electroporation. (a) Upon application to the microelectrode of a train of 10 ms wide pulses (1.3 V amplitude), large potential transients developed in the cell (arrow) (cut off at ±100 mV), thus causing the opening of membrane pores by electroporation. Pores opening shunted the intracellular potential (initially at a resting value of about −70 mV) to the zero potential of the grounded electrolyte. (b) Serial electroporation. Where indicated by arrows, voltage transients were applied to the microelectrode as in (a), thereby inducing a repetitive electroporation of the single cell. At each electroporation event, the intracellular potential shifted from the resting potential (−70 mV) to a higher potential. This was zero for the first two electroporations and was followed by recovery to resting potential within about 1–1.5 min. With the third electroporation, the potential transition was less pronounced (to only about −30 to −40 mV) and the recovery to the resting potential was slower as possible consequences of partial cell detachment from the substrate and membrane damage.

Tunable delivery by single-cell electroporation: from small polar molecules to nucleic acids

We assessed the possibility to finely tune the delivery of polar molecules to single CHO-K1 cells, from small probe compounds to nucleic acids. As probe compounds, in addition to LY, we chose the larger chromophore Trypan Blue (TB) (MW 892 Da) and a single-stranded fluorescein labeled 24 nt ODN. We used a voltage protocol composed by three trains of five 10 ms wide pulses (trains spaced by 100 ms). We observed the efficiency of delivery of the three different compounds for pulse amplitudes of 0.9, 1.3 and 1.7 V. Each voltage was tested and the efficiency estimated in four independent experimental trials ($n = 4$) of 100 cell–microelectrode contact sites each ($N = 100$). Interestingly, by simply varying the amplitude of the applied voltage pulses, we were able to tune the membrane permeability to the different compounds (Figure 4).

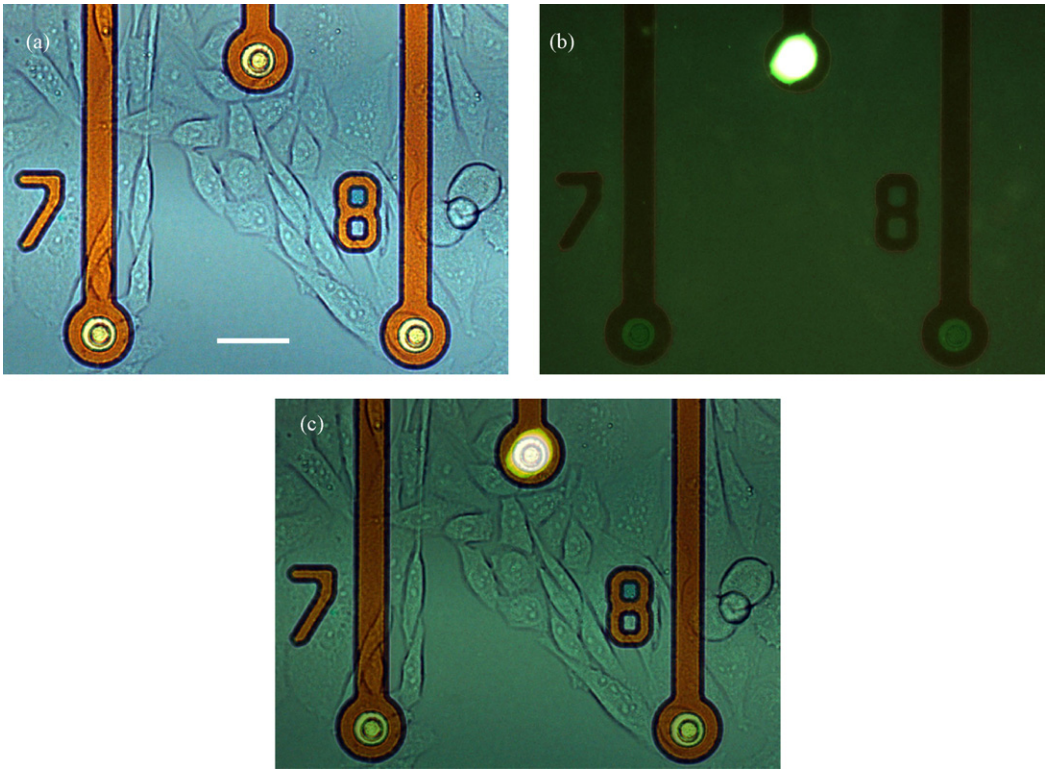

FIGURE 3

Delivery of LY to CHO-K1 cell by single-cell electroporation. Brightfield (a) and fluorescence micrograph (b) of a single cell-on-microelectrode demonstrating the uptake of the dye LY after electroporation. After selecting the corresponding electrode through the control system (electrodes 7 and 8 were not selected), the cell was electroporated in the presence of LY in the extracellular solution (1 mM). After 1 min incubation and washing with PBS, only the electroporated cell was stained, thus demonstrating the permeabilization of the membrane due to the opening of transient pores. (c) Merged image of (a) and (b). Electroporation voltage protocol: 3 trains of 5, 10 ms wide, voltage pulses spaced by 100 ms (1.6 V amplitude). Scale bar in a: 15 μm (a–c).

Below 0.9 V, no uptake occurred for any of the compounds. Above 0.9 V, increasing the voltage amplitude led to an increase in transfection efficiency for LY and TB, although the membrane remained impermeable to the ODN up to 1.3 V. Above the 1.3 V threshold, a new permeability transition occurred with the uptake efficiency of ODN that was reaching 80% at 1.7 V. At this voltage, the efficiency of delivery for LY and TB was 100%. These results can be probably interpreted considering the effect of increasing the voltage on pores number and/or diameter [28,29]: the higher the voltage, the larger was the number and/or diameter of the pores in the cell membrane, thereby increasing the efficiency of delivery for the molecules with higher molecular weight.

Cell viability with different voltage protocols was also investigated to check the effect of increasing the voltage amplitude on cell survival. As reported in Figure 4, cell viability at 24 h decreased at higher voltages, although the percentage of viable cells was very satisfactory when compared to conventional electroporation methods on cell populations in cuvettes. Noteworthy, we simply acted in these experiments only on the pulse amplitude and used a conventional PBS buffer. Several other electroporation parameters are suitable for custom adjustments, such as the shape of voltage transients [30] or the osmolarity of the bath solution [31] and its ionic composition [20]. Careful optimization of all these parameters can be used to further improve the single-cell electroporation array capabilities to tune molecular delivery for a variety of compounds and to different cell types.

Space-resolved single-cell delivery

One major feature of the single-cell electroporation array is that electroporation can be easily performed at different sites in the same culture by pre-selecting the single cells via the computer driven control system (space-resolved electroporation). As a proof of principle experiment, we activated nine different electrodes in contact with CHO-K1 cells and performed a spatially resolved delivery of TB to draw a triangle with the electroporated cells (Figure 5). Upon electroporation, incubation with TB and washing, cells in contact with the electrodes were stained. Only a few cells randomly distributed over the large inter-electrodes area showed off-site uptake, thus demonstrating a high specificity of space resolved electroporation. A larger space-resolved experiment where a single-stranded fluorescent ODN was delivered is shown in Figure 6. The experiments demonstrated that delivery of small drug-like molecules and nucleic acids could be effectively achieved at different sites of the same culture, and we confirmed these results with different arbitrarily chosen combinations of electrodes (not shown). The possibility that off-site non-specific uptake was induced by the single-cell electroporation process was excluded by statistical analysis of different delivery experiments with the three probe compounds: LY, TB and ODN (Table 1). The non-specific uptake index, NS, representing the ratio of off-site and site-specific cell staining as described in the Material and Methods, was determined for four experimental trials of 100 cell–microelectrode sites for each compound. From Table 1, it is clear that, on average, only

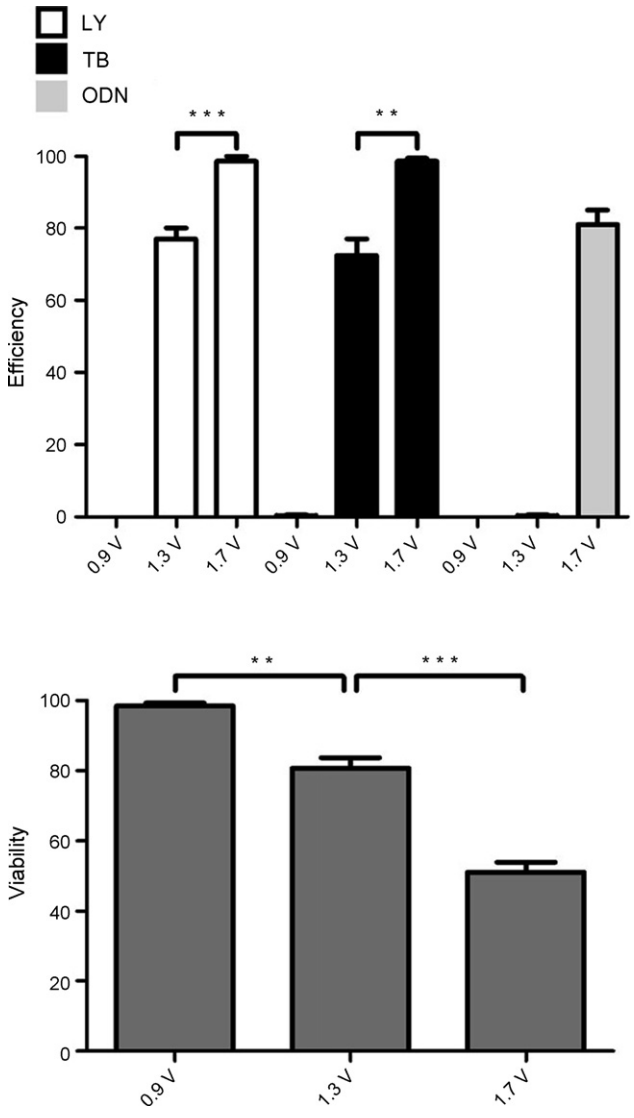

FIGURE 4

Effect of pulse amplitude on the efficiency of delivery. (Top) Efficiency of delivery to CHO-K1 cells for three different probe compounds, LY, TB and 24 nt fluorescein labeled ODN and for three different pulse amplitudes. Efficiency, which is expressed as percentage in the diagram, was computed for four different experimental trials, each of 100 cell–microelectrode sites, as described in the Materials and Methods. Electroporation protocol: 3 trains of 5, 10 ms wide, voltage pulses spaced by 100 ms. With pulse amplitudes up to 0.9 V, none of the probe molecules was delivered. By increasing the voltage above this threshold, the membrane was made progressively more permeable to LY and TB, but not to ODN, until a new threshold was reached (1.3 V). Further increasing the pulse amplitude, induced a corresponding increase of membrane permeability particularly with respect to ODN, with delivery efficiency reaching about 80% at 1.7 V. (Bottom) Cell viability was tested by TB assay at 24 h. A simple PBS solution was used in order to prevent cytotoxic effects of the probe compounds from affecting the viability estimate. All data represent mean ± S.D. ($n = 4$). $^{**}P < 0.01$, $^{***}P < 0.001$, not indicated where $P \ll 0.001$.

10.9–17.5 off-site non-specifically stained cells were found for every 100 on-site cells with specific uptake. Considering that the inter-electrodes area where off-site cells were counted was much larger than the area of the microelectrodes, this number demonstrates the high specificity of space resolved single-cell electroporation. Similar numbers of cells with off-site uptake were

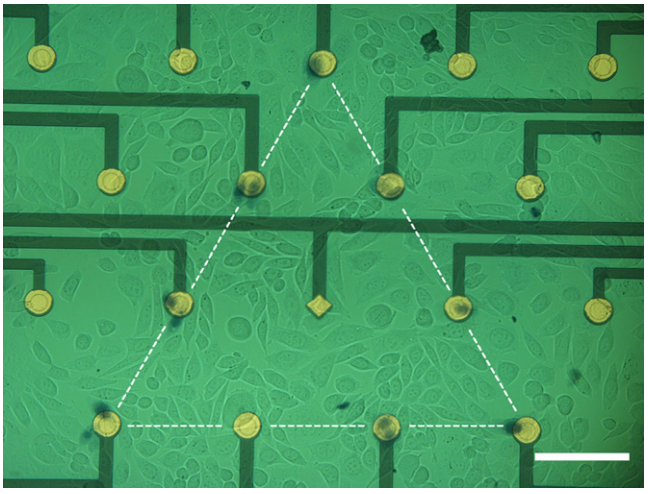

FIGURE 5

Space resolved delivery of TB. Space-resolved delivery of TB was used to draw a triangle with the target cells. Nine electrodes of the microarray were selected through the PC driven control system to draw a triangle (dashed line). After electroporation in the presence of TB, incubation for 1 min and washing, the cells growing on pre-selected electrodes were stained. Only rare randomly distributed cells showed off-site uptake, probably because of spontaneous cell death or duplication. Electroporation voltage protocol as in Figure 3. Scale bar 100 μm.

obtained from non-electroporated cultures on chip (not shown), thus showing that non-specific uptake is due to normal death or duplication processes that are randomly occurring within the cell population in culture. Space-resolved single-cell delivery is particularly intriguing for its screening perspectives: using the single target cells on a chip as individual 'test tubes', it becomes possible to assess different molecules by parallel single-cell experiments under the same culture conditions. In complex cultures, where cells of different type are communicating by cell–cell signaling events, space-resolved cell targeting will enable to investigate cell–cell signaling with unprecedented resolution as, for example, in primary cultures of neurons.

Time-resolved and serial delivery

Delivery of molecules could be easily operated in a time-resolved manner: since the different target cells were independently addressed, molecules could be delivered at arbitrarily chosen time points. One major advantage of time-resolved delivery is the possibility to sequentially introduce molecules into the same cell (serial delivery). First, serial electroporation was investigated both electrophysiologically and by the uptake of probe compounds. While monitoring the intracellular potential with a patch-clamp pipette, we could induce membrane electroporation several times, followed by pores resealing and recovery of the cell potential (Figure 2b). Using appropriate electroporation protocols and provided that an interval of at least ten minutes was left between successive electroporations, we did not observe any electrophysiological sign of cell damage. When this interval was shortened below the ten minutes, the cell potential was more slowly, and often not completely, recovering after the second or third electroporation (Figure 2b), suggesting that at least ten minutes are required for pores resealing and full cell recovery. We checked for serial transfection of CHO-K1 cells using the single-stranded

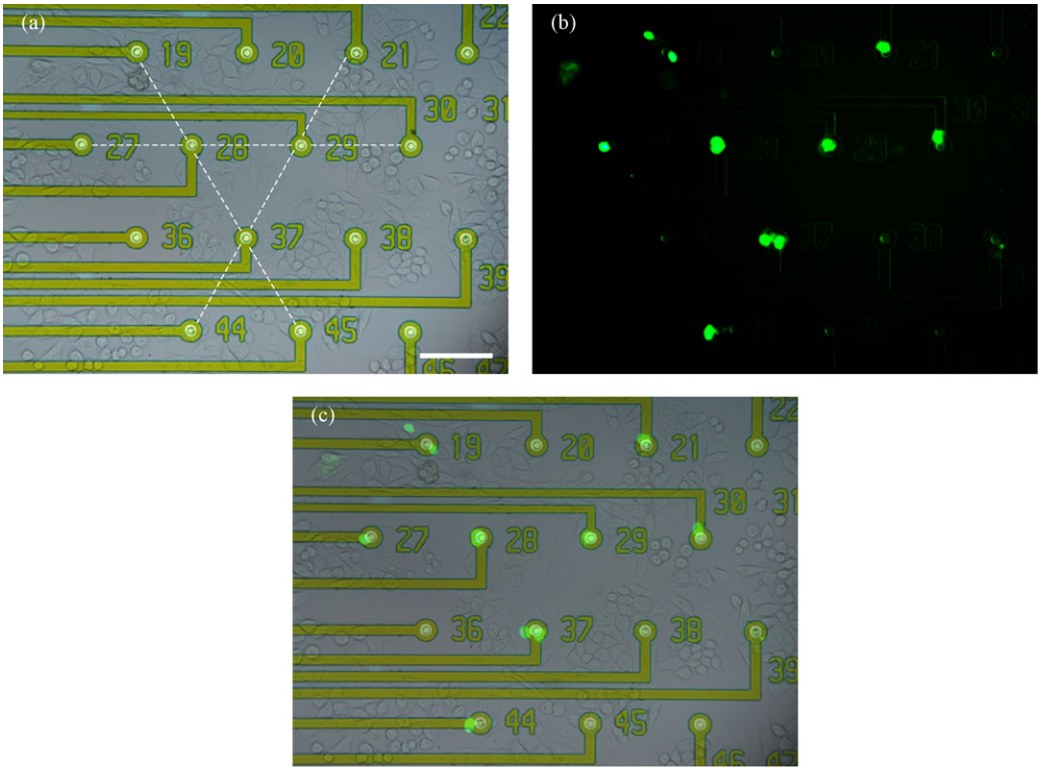

FIGURE 6

Space-resolved delivery of ODN. Space-resolved delivery of a 24 nt fluorescein labeled single stranded ODN. (a) Brightfield and (b) fluorescence micrographs. (c) Merged (a) and (b) image. Nine different electrodes (19, 21, 27, 28, 29, 30, 37, 44, 45) covered by CHO-K1 cells were selected for electroporation in order to draw a geometrical pattern (dashed line). After 10 min incubation and washing, all of them except electrode 45 showed ODN internalization, thus demonstrating the possibility to deliver these nucleic acids to arbitrarily pre-selected cells within the same culture and with high efficiency. Particularly in the merged image, it is recognizable the tendency of the ODN to accumulate in the cell nucleus. Voltage protocol as in Figure 3. Scale bar in a: 100 μm (a–c).

fluorescein labeled ODN as probe nucleic acid (Figure 7). The figure shows that three hours after the first delivery, the nuclear fluorescence due to the ODN uptake had vanished. A second incubation with ODN not coupled to electroporation demonstrated that the resealing of pores had occurred and, with a second electroporation, the ODN could be delivered again to the same cell. Thus, according to our experiments, serial delivery of nucleic acids can be achieved with a time resolution of only a few minutes, thereby opening the possibility to finely control the dynamics of gene expression events with exogenous molecular tools in high-resolution time-resolved experiments. Notable was the nuclear localization of the ODN after single-cell electroporation that was also confirmed for a 24 bp fluorescein labeled double-stranded ODN (not shown). In fact, frequently ODNs need to reach the nucleus to

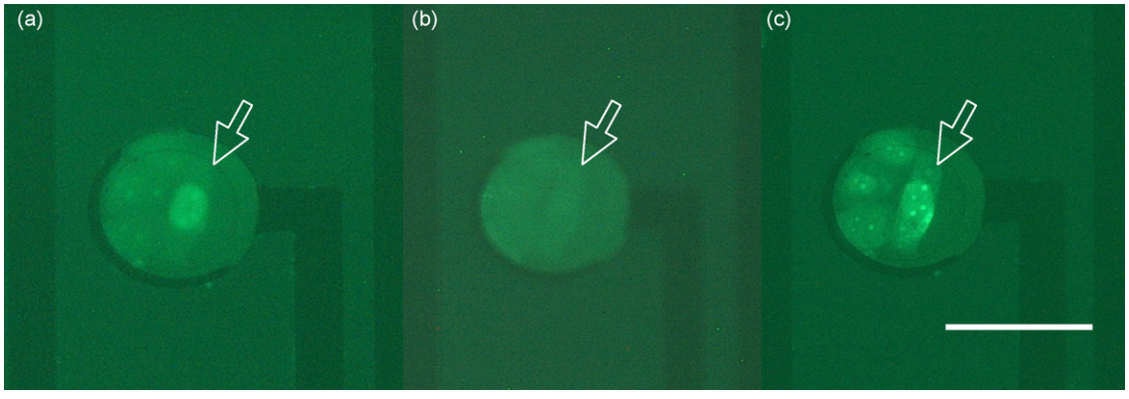

FIGURE 7

Serial transfection with ODN. Serial transfection of a target cell with the fluorescein labeled 24 nt ODN. From left to right: (a) the first transfection by single-cell electroporation induced the nuclear uptake of the ODN (white arrow indicating the cell nucleus). (b) Three hours later, the fluorescence had vanished. Following a second incubation with the ODN no uptake was observed, thus demonstrating that membrane pores had resealed. By a second electroporation (c), the ODN was delivered again to the same cell. Note that large 50 μm electrodes were used in this experiment and that more than one cell on the target electrode was displaying ODN uptake after the second electroporation. Voltage protocol: 3 trains of 5, 10 ms wide pulses spaced by 100 ms. Pulse amplitudes: 1.7 and 1.5 V for the first and the second electroporation, respectively. Scale bar in c: 50 μm (a–c).

exert their action as, for example, double-stranded decoy ODNs, which is not easily achievable by usual chemical transfection methods due to compartmentalization of the nucleic acids within the cell cytosol [16]. Our observation is consistent with the nuclear localization of ODNs that was previously reported by using a standard electroporation approach [32].

Single-cell space and time-resolved gene expression and silencing

We tested the technique for single-cell gene expression experiments in CHO-K1 cells by delivering a plasmid vector, for gene expression, and a siRNA, for gene silencing. Figure 8 shows the result of single-cell transfection of CHO-K1 cells with a plasmid encoding EGFP. To this purpose, we used a short-pulse (100 μs wide) based voltage protocol, which was inspired to a protocol for plasmid transfection by conventional electroporation [20]. We achieved, so far, a transfection efficiency of 46% ($N = 61$), although further optimization of the voltage protocols, buffer solutions and other electroporation parameters will probably lead to further improvement.

Delivery of siRNA was first proven to work with high efficiency (about 80% as in the case of the 24 nt single-stranded ODN) using control fluorescent siRNA (not shown). Thus, we performed silencing experiments on CHO-K1 cells stably transfected with the ECFP gene using a specific siRNA [24]. After delivering the siRNA by single-cell electroporation, we expected to observe a decrease of fluorescence in the target cells due to the silencing of the ECFP gene. Control experiments with a standard bulk-scale method (Metafectene transfection reagent) for siRNA delivery, confirmed the capability of the siRNA to silence the ECFP gene inducing a randomly distributed but significant (40–100%) decrease of fluorescence within the cell population after 24–48 h (not shown). A target site on the single-cell electroporation array 48 h after siRNA transfection is visible in Figure 9. By comparing the brightfield and fluorescence images, it is clear that two cells, one covering the microelectrode and the other one in its immediate proximity (white arrows), showed a dramatic decrease of fluorescence intensity. The result can be explained considering that the two cells were probably deriving from duplication of the target siRNA-transfected cell and that the site-specific delivery of siRNA induced ECFP silencing. The efficiency of ECFP silencing was quite low so far (8%; $N = 100$). This was somehow in contrast with the high efficiency of transfection obtained both with ODNs and fluorescent control siRNA (80%) and with the good ECFP silencing efficiency (>40%) achieved using the Metafectene transfection reagent in control experiments on populations of cells. We may argue that, owing to the high efficiency of delivery by single-cell electroporation, the intracellular concentration reached by the siRNA in the target cells was too high, thus causing cytotoxic side effects [33]. An alternative hypothesis is that siRNA accumulation in the nucleus was lowering the siRNA concentration in the cytoplasm below the working level. It is reasonable to assume that the silencing efficiency will be improved by carefully tuning the electroporation protocol and the siRNA extracellular

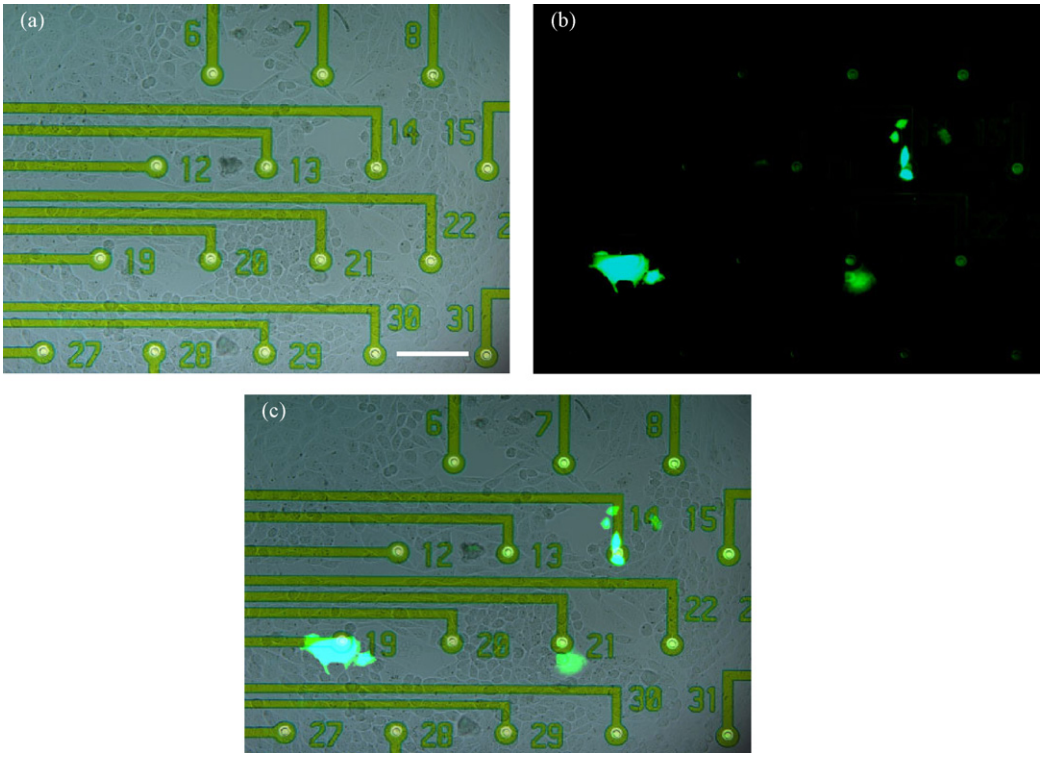

FIGURE 8

Space-resolved gene expression. Brightfield (**a**) and fluorescence (**b**) micrographs showing the space-resolved transfection of CHO-K1 cells with a plasmid encoding for EGFP. (**c**) Merged image of a and b. Cells were observed 24 h after transfection by single-cell electroporation (pre-selected electrodes: 8, 12, 13, 14, 19, 21, 27, 28, 29). Visible is the typical EGFP fluorescence of a single transfected cell (electrode 21) or of a few cells (electrodes 14 and 19) originating from replication of single target cells. Voltage protocol: first short 100 μs pulse of 4 V followed by a decreasing pulsed ramp, 100 ms long, starting from 1 V. Scale bar in a: 100 μm (a–c).

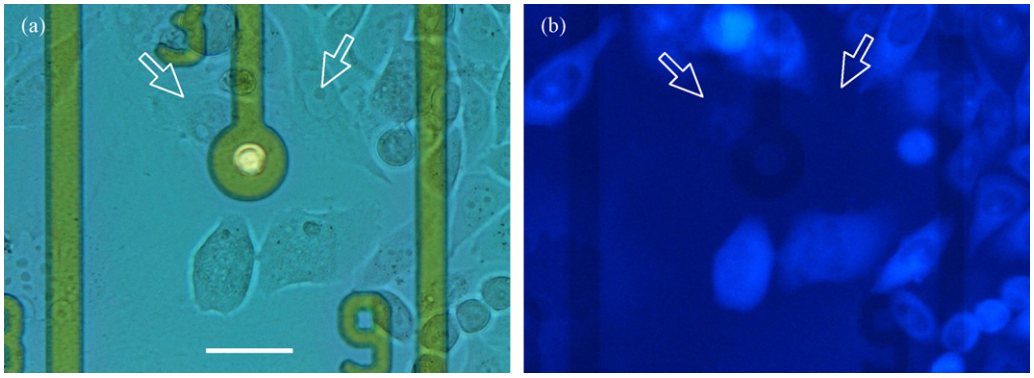

FIGURE 9

siRNA mediated gene silencing. Brightfield (a) and fluorescence (b) micrographs showing ECFP silencing 48 h after siRNA delivery by single cell electroporation. CHO-K1 cells stably transfected with the ECFP gene were used. Cells covering the electrode and in its immediate proximity (arrows) were showing ECFP silencing. The cells were deriving from the replication of one target cell transfected with siRNA. It is clear the disappearance of the ECFP fluorescence in the cytoplasm, which is conserved by all the other non-electroporated cells in culture. Scale bar in a: 15 μm (a–b).

concentration in order to reach the appropriate siRNA level in the cell cytoplasm.

We assessed the new technique for the serial expression of two reporter genes in a single CHO-K1 cell. Figure 10 shows the result of a serial expression first of EYFP and then of ECFP. At 24 h from the first transfection with the EYFP plasmid, the target cell showed the typical cytoplasmic fluorescence. The cell was then transfected a second time with ECFP. After 24 h (48 h from the first transfection with EYFP) cell replication had occurred and double expression of EYFP and ECFP was visible in the daughter cells. We reached an efficiency of serial transfection with two reporter genes of 45% ($N = 141$), which is reasonable considering that some cells were moving out of the electrode area after the first transfection and could not be electroporated twice.

Discussion

We have developed a new on-chip single-cell electroporation technology enabling the delivery of impermeant compounds to pre-selected individual mammalian cells in culture. Controlled by an easy-to-use PC driven control system, a single-cell electroporation array based on cell-sized planar microelectrodes was used to perform a tunable, space- and time-resolved transfection of individual CHO-K1 cells. Target cells were directly addressed while growing in adhesion on the solid substrate of the chip, thus avoiding harmful detachment and re-suspension treatments. The method was proved to be tunable: by simply acting on the amplitude of the voltage transients applied to the microelectrodes, the efficiency of delivery was modulated for molecules with different molecular weight, from small dyes to antisense-like ODNs. Space and time-resolved delivery of molecules were implemented. Pre-selected individual cells were transfected at different sites of the same culture (space-resolved) and at arbitrarily chosen time points (time-resolved). Time-resolved electroporation of the cell membrane was investigated by an electrophysiological approach. It was proven that the same cell can be repeatedly electroporated within a time-scale of a few minutes and that oligonucleotides and plasmid vectors can be delivered to the same cell at different time points (serial delivery). The applicability of the approach to the investigation of gene expression events in cultured mammalian cells was demonstrated through proof-of-principle experiments with fluorescent reporter genes. The silencing of a fluorescent protein gene by delivery of siRNA was achieved in target cells as well as its expression by a DNA plasmid vector. The serial transfection of the same cell with two different fluorescent proteins was also obtained. Thanks to the on-chip implementation and to the PC driven control system, single-cell space and time-resolved delivery experiments could be performed extremely easily and without the need of special skills.

The technique represents a clear advance with respect to other state-of-the art cell microarrays [34–37]. First of all, it allows delivery to single cells while conventional cell microarrays work on cell populations. Then, it enables delivery to be performed at arbitrarily chosen time-points and to be repeated to the same cells, compared to the one-shot-only previous cell microarrays approaches. Since the method is based on electroporation, which is 'per se' a tunable way to regulate membrane permeability to exogenous compounds, delivery of other impermeant molecules in addition to nucleic acids can be obtained as we have demonstrated by delivering of polar dyes. Also taking advantage from the fine tuning at the single-cell level of the electroporation protocol, it is likely that the method will be broadly applicable across a range of molecules, from small dyes to proteins and nucleic acids, and cell types, from cell lines to primary cultures. This idea is supported by our own preliminary experimental tests (unpublished results) and by previous results of '*in situ*' electroporation [21].

With respect to other non-on-chip single-cell delivery methods such as microinjection, carbon fibers or glass capillaries-mediated electroporation [22] and photoporation [38], the technique is extremely easy to use and, most importantly, it is suitable for future lab-on-chip integration with other micro- and nano-scale cell analysis techniques [39]. To this respect, it should be noted that cell-sized planar metal electrodes have been used for many years for recording and stimulation of the electrical activity of excitable cells in culture [40]. The approach could be now coupled to molecular delivery and genetic manipulation. As drawbacks, however, we must point out that the density of the microelectrodes limits space resolution, that the technique can be applied only to cultures and not to cells in a tissue and that epi-illumination has to be used for cell observation because the silicon substrate of the chip is not transparent. Compared to manual microinjection, which is up to now the most

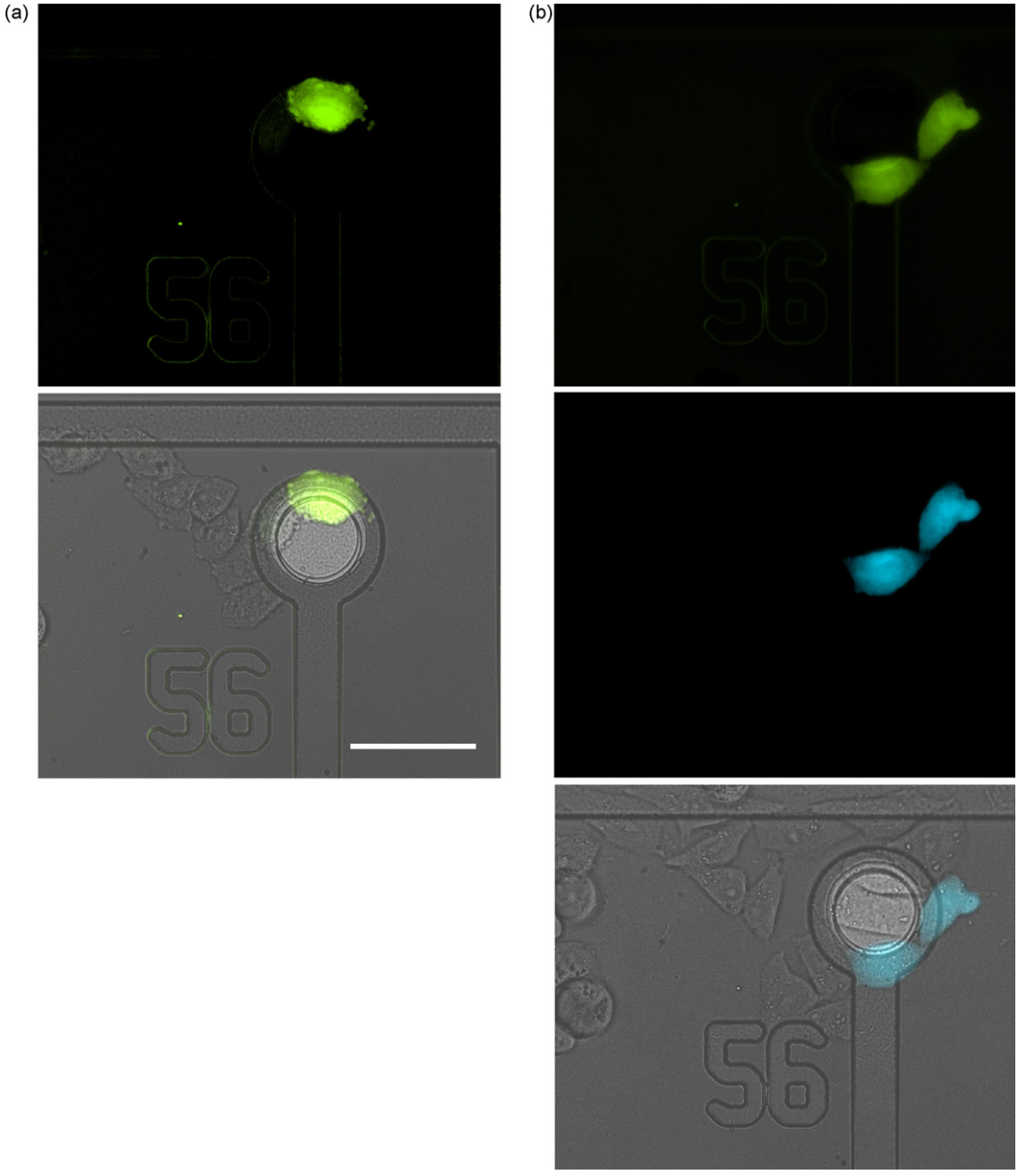

FIGURE 10

Serial transfection of EYFP and ECFP. Panel a: 24 h after the first transfection with the EYFP plasmid the target cell shows the typical yellow fluorescence. Fluorescence micrograph (top). Merged image of Brightfield and fluorescence micrographs (middle). Panel b: the same target cell was transfected a second time with ECFP. 24 h after this second electroporation, two cells deriving from the duplication of the target cell were detected expressing both EYFP (top) and ECFP (middle). *Bottom*: merged image of the Brightfield with the ECFP fluorescence micrographs. Voltage protocol: 50 ms wide sinusoid, 3 V amplitude. Scale bar: 15 μm (panels a and b).

standardized and widespread method for single-cell delivery, the new technique offers major advantages: (i) it does not require any special operator skill, thus making the method easily adoptable by any laboratory; (ii) it is much faster, thanks to the high time resolution, allowing for molecular delivery in parallel or in sequence to a number of single cells within a few minutes; (iii) it is tunable, since by acting on the electroporation protocol the size of the molecule to be delivered and the degree of membrane damage can be finely regulated (iv) it enables serial delivery to the same cell with a resolution limit of only about ten minutes, at least according to our electrophysiology measurements; (iv) it is suitable for high-throughput implementations, since the number of electrodes can be largely increased by standard semiconductor technology. To this respect, it should be pointed out that automated microinjection systems have been developed where the injector is driven to the cells by a robotic arm ([41]; www.fujitsu.com/downloads/SOL/bsg/cellinjector.pdf). Considering that approaching and perforating the cell is a complex and very delicate procedure, we may expect our method to be more versatile and tunable for different cell types, besides representing a low-cost alternative. As drawbacks, at present, we should mention the impossibility of using inverted microscopes and the low space resolution of the actual

microelectrodes array (150–300 μm inter-electrodes distance). Both aspects, however, are suitable for improvements as reported below.

Finally, in comparison to other previous attempts to implement single-cell electroporation on-chip, our method allows for direct electroporation of cells growing in adhesion and does not require cell harvesting and positioning in microchambers or microfluidic channels. In addition, it relies on a much simpler fabrication technology, which represents a clear advantage for future lab-on-chip integration with other techniques.

Overall, the method offers a variety of application perspectives since the type of molecule, the timing of delivery and, perhaps, even the intracellular concentration, become freely tunable parameters for a number of individual target cells within the same culture. On its basis, new experimental paradigms relying on the combination of molecular manipulation and analysis techniques could be easily implemented at the single cell level *in vitro*.

Our results offer proof-of-principle evidence of these possibilities, but optimizations are obviously required for the single applications. A combination with surfection approaches [36] can be foreseen. However, it should be noted that optimization (and customization) might rely both on adjustments of electroporation conditions and on further chip developments. Electroporation can be set for efficient delivery of a large variety of molecules and to very different cell types by acting on several parameters, from the voltage shape and amplitude to the solution composition [20]. On the chip side, by taking advantage of semiconductor technology, the platform is suitable for many improvements, as for example, by increasing the number and density of the electroporation sites to facilitate serial delivery or for high-throughput screening applications. The integration with microfluidic channels [39] will allow for a customized perfusion and analysis of compounds directly onto the target cells of the array and the substitution of the bulk silicon with transparent substrates will make the array compatible with the use of inverted microscopes (possibly complemented by the use of transparent microelectrodes). Notably, however, observation can be already performed by epi-illumination and the method may be easily implemented for single-molecule and time-lapse fluorescence microscopy experiments in single living cells [8–12]. Its integration with 'high-throughput' screening devices [42,43] and with on-chip techniques for single-cell analysis at the genetic, chemical and morphological level [39,44] will pave the way to new large-scale automated experimental tools.

A number of future applications in genetic research can be envisaged, spanning from functional genomics to drug discovery: time-resolved gene expression studies [3,11], siRNA screenings [45], pre-clinical identification and testing of new gene therapy strategies based on nucleic acids [46] and many others. By taking advantage of serial electroporation, the technology may enable better assessment of time-dependent molecular mechanisms, such as those controlling the dynamics of gene expression in genetic regulatory networks of mammalian cells. By means of space-resolved delivery, genetic and molecular manipulation of individual cells interacting within the same culture may be easily performed, thus facilitating the investigation of cell–cell signaling mechanisms. For example, neuron–neuron communication may be investigated by individual expression and silencing of genes involved in synaptic plasticity. Overall, the combination of time-resolved and space-resolved single-cell delivery promises to open new experimental perspectives in the area of systems biology where complex cell systems *in vitro* have to be investigated at the molecular level. With respect to industrial applications, the technique may be implemented into automated lab-on-chips for multi-sample assays in high-throughput drug screening and microkinetics studies or for the generation and selection of cell clones used in bioreactors based on mammalian cells [47].

Acknowledgements

We thank Prof. C. Reggiani for critical reading of the manuscript and Prof. P. Fromherz for discussion and suggestions. This work was supported partly by a PRIN research grant from the ''Ministero della Ricerca Scientifica e Tecnologica'' of Italy. The manuscript is dedicated to the memory of Dr. Silvano Fumero, who has given this work a constant support, with enthusiasm and determination.

References

1 Raser, J.M. and O'Shea, E.K. (2005) Noise in gene expression: origins, consequences, and control. *Science* 309, 2010–2013
2 Rosenfeld, N. *et al.* (2005) Gene regulation at the single-cell level. *Science* 307, 1962–1965
3 Longo, D. and Hasty, J. (2006) Dynamics of single-cell gene expression. *Mol. Syst. Biol.* 2, 64
4 Lahav, G. *et al.* (2004) Dynamics of the p53-Mdm2 feedback loop in individual cells. *Nat. Genet.* 36, 147–150
5 Nelson, D.E. *et al.* (2004) Oscillations in NF-kappaB signaling control the dynamics of gene expression. *Science* 306, 704–708
6 Peixioto, A. *et al.* (2004) Quantification of multiple gene expression in individual cells. *Genome Res.* 14, 1938–1947
7 Hinkle, D. *et al.* (2004) Single neurons as experimental systems in molecular biology. *Progr. Neurobiol.* 72, 129–142
8 Cai, L. *et al.* (2006) Stochastic protein expression in individual cells at the single-molecule level. *Nature* 440, 358–362
9 Giepmans, B.N.G. *et al.* (2006) The fluorescent toolbox for assessing protein location and function. *Science* 312, 217–224
10 Sako, Y. (2006) Imaging single molecules in living cells for systems biology. *Mol. Syst. Biol.* 1, 56
11 Shav-Tal, Y. *et al.* (2006) Gene expression within a dynamic nuclear landscape. *EMBO J.* 25, 3469–3479
12 Xie, X.S. *et al.* (2006) Living cells as test tubes. *Science* 312, 228–230
13 Gingsberg, S.D. (2005) RNA amplification strategies for small sample populations. *Methods* 37, 229–237
14 Hartmann, C.H. and Klein, C.A. (2006) Gene expression profiling of single cells on large-scale oligonucleotide arrays. *Nucleic Acids Res.* 34, e143
15 Liu, B.-F. *et al.* (2006) Micro-separation toward systems biology. *J. Chromatogr. A* 1106, 19–28
16 Bene, A. *et al.* (2004) Subcellular localization as a limiting factor for utilization of decoy oligonucleotides. *Nucleic Acids Res.* 32, e142
17 Urnov, F.D. *et al.* (2005) Highly efficient endogenous human gene correction using designed zinc-finger nucleases. *Nature* 435, 646–651
18 Porteus, M.H. and Carroll, D. (2005) Gene targeting using zinc finger nucleases. *Nat. Biotechnol.* 23, 967–973
19 Durai, S. *et al.* (2005) Zinc finger nucleases: custom-designed molecular scissors for genome engineering of plant and mammalian cells. *Nucleic Acids Res.* 33, 5978–5990
20 Gehl, J. (2003) Electroporation, theory and methods, perspectives for drug delivery, gene therapy and research. *Acta Physiol. Scand.* 177, 437–447
21 Arulanandam, R. *et al.* (2005) Transfection techniques affecting Stat3 activity levels. *Anal. Biochem.* 338, 83–89
22 Olofsson, J. *et al.* (2003) Single-cell electroporation. *Curr. Opin. Biotechnol.* 14, 29–34

23 Kovacs, G. (1994) Introduction to the theory, design and modeling of thin-film microelectrodes for neural interfaces. In *Enabling Technologies for Cultured Neural Networks* (Stenger, D.A. and McKenna, T., eds), pp. 121–166, Academic Press

24 Caplen, N.G. *et al.* (2001) Specific inhibition of gene expression by small double-stranded RNAs in invertebrate and vertebrate systems. *Proc. Natl. Acad. Sci.* 98, 9742–9747

25 Gleixner, R. and Fromherz, P. (2006) The extracellular electrical resistivity in cell adhesion. *Biophys. J.* 90, 2600–2611

26 Bandiera, L. *et al.* (2006) Electrical modeling of a biochip for genetic manipulation of single cells. *IEDM Proc.* 723–726

27 Ghosh, P.M. *et al.* (1993) Monitoring electropermeabilization in the plasma membrane of adherent mammalian cells. *Biophys. J.* 64, 1602–1609

28 Neumann, E. *et al.* (1999) Fundamentals of electroporative delivery of drugs and genes. *Bioelectrochem. Bioenerg.* 48, 3–16

29 Smith, K.C. *et al.* (2004) Model for creation and evolution of stable electropores for DNA delivery. *Biophys. J.* 86, 2813–2826

30 Kotnic, A. *et al.* (2003) Role of pulse shape in cell membrane electropermeabilization. *Biochim. Biophys. Acta* 1614, 193–200

31 Golzio, M. *et al.* (1998) Control by osmotic pressure by voltage-induced permeabilization and gene transfer in mammalian cells. *Biophys. J.* 74, 3015–3022

32 Liu, Y. and Bergan, R. (2001) Improved intracellular delivery of oligonucleotides by square wave electroporatioin. *Antisense Nucleic Acid Drug Dev.* 11, 7–14

33 Scherer, L.J. and Rossi, J.J. (2003) Approaches for sequence-specific knockdown of mRNA. *Nat. Biotechnol.* 21, 1457–1465

34 Ziauddin, J. and Sabatini, D.M. (2001) Microarrays of cells expressing defined cDNAs. *Nature* 411, 107–110

35 Baghdoyan, S. *et al.* (2004) Quantitative analysis of highly parallel transfection in cell microarrays. *Nucleic Acids Res.* 32, e77

36 Chang, F.-H. *et al.* (2004) Surfection: a new platform for transfected cell arrays. *Nucleic Acids Res.* 32, e33

37 Yamauchi, F. *et al.* (2004) Spatially and temporally controlled gene transfer by electroporation into adherent cells on plasmid DNA-loaded electrodes. *Nucleic Acids Res.* 32, e187

38 Paterson, L. *et al.* (2005) Violet diode-assisted photoporation and transfection of cells. *Biopharm. Int.* 18, 30–35

39 El-Ali, J. *et al.* (2006) Cells on chips. *Nature* 442, 403–411

40 Rutten, W.L.C. (2002) Selective electrical interfaces with the nervous system. *Annu. Rev. Biomed. Eng.* 4, 407–452

41 Yao, J. *et al.* (2002) Coordination of mesangial cell contraction by gap junction-mediated intercellular Ca^{2+} wave. *J. Am. Soc. Nephrol.* 13, 2018–2026

42 Lang, P. *et al.* (2006) Cellular imaging in drug discovery. *Nat. Rev. Drug Discov.* 5, 343–356

43 Rausch, O. (2006) High content cellular screening. *Curr. Opin. Chem. Biol.* 10, 1–5

44 Andersson, H. and van den Berg, A. (2004) Microtechnologies and nanotechnologies for single-cell analysis. *Curr. Op. Biotechnol.* 15, 44–49

45 Moffat, J. and Sabatini, D.M. (2006) Building mammalian signaling pathways with RNAi screens. *Nat. Rev. Mol. Cell. Biol.* 7, 177–187

46 Proske, D. *et al.* (2005) Aptamers-basic research, drug development, and clinical applications. *Appl. Microbiol. Biotechnol.* 69, 367–374

47 Wurm, M. (2004) Production of recombinant protein therapeutics in cultivated mammalian cells. *Nat. Biotech.* 22, 1393–1398

48 Andrieu-Soler, C. *et al.* (2005) Stable transmission of targeted gene modification using single-stranded oligonucleotides with flanking LNAs. *Nucleic Acids Res.* 33, 3733–3742